FKN regulates macrophage activation in lupus nephritis via the Hippo signaling pathway

Yao Zuo
First Affiliated Hospital of Jinan University
Xiuhong Pan
Affiliated Hospital of Youjiang Medical University for Nationalities
Xiaochao Wang
Affiliated Hospital of Youjiang Medical University for Nationalities
Yanwu You (youyanwu@163.com)
First Affiliated Hospital of Jinan University

Research Article

Keywords: Lupus nephritis, Fractalkine, Macrophage, Polarization, Hippo signaling pathway

Posted Date: August 3rd, 2022

DOI: https://doi.org/10.21203/rs.3.rs-1722971/v1

Abstract

Introduction: Lupus nephritis (LN) is a serious complication of systemic lupus erythematosus (SLE), and its pathogenesis is not fully understood. There is an imbalance in the polarization of macrophages and an interplay between fractalkine (FKN) and its receptor, CX3CR1, in LN. Previously we showed that the expression levels of FKN were positively correlated with the severity of LN. Here we aimed to study the role of the Hippo signaling pathway (HSP) and its interaction with FKN in LN in an attempt to provide novel strategies for the treatment of this condition.

Methods: 91 LN patients and 64 healthy controls were included in this study. In addition, FKN-knockout mice and RAW.267.4 cells were used for *in vivo* and *in vitro* experiments. The levels of YAP, TAZ, MST1, IL-6, and IL-10 were measured in LN patients by qRT-PCR and ELISAs. HE, Masson and PASM staining were used to assess the pathological changes in kidney tissues and western blots measured the protein content of FKN, MST1, YAP, p-YAP, p-TAZ, iNOS, TNF-α, IL-10 and Arg-1. IF was used to localize F4/80, F4/80, p-YAP, IL-10 and TNF- α proteins.

Results: Up-regulation of FKN was associated with increased macrophage activation and increased YAP expression. When FKN was down-regulated the HSP was activated and the YAP expression was decreased. In addition, macrophages polarization switched to M1-phenotype. Activation of the HSP *in vivo* was associated with FKN deficiency and increased phosphorylation of YAP and TAZ, leading to reduced activation of macrophages. This could relieve the renal damage associated with LN.

Conclusions: Our results confirmed a negative correlation between the FKN gene and the HSP. Down-regulation of FKN could activate the HSP to reduce the activation of macrophages in kidney tissues and attenuate renal damage. The HSP may provide a new molecular target for the treatment of LN patients.

Introduction

Systemic lupus erythematosus (SLE) is an autoimmune syndrome caused by abnormal immune responses, which is characterized by the production of antibodies against self-antigens, the formation of immune complex deposits, activation of B cells and T cells and excessive release of inflammatory factors[1]. The physiological function and system of the host body can be influenced by SLE, including the skin, muscles, heart, nervous system and kidneys. The involvement of the kidneys is manifested as lupus nephritis (LN). The main clinical characteristics of LN are proteinuria, hematuria and varying degrees of renal damage, which are the most serious complications of SLE. The high death rate of patients is mainly caused by these side effects[2]. However, there is still lack of effective therapy for LN. Traditional treatments are mainly dependent on chemotherapy, which include the use of immune suppressants and glucocorticoids. Nevertheless, these have numerous side effects and are difficult to be accepted by patients. Due to the indistinct pathogenesis of LN, there is still a major need to explore potential new clinical treatments for patients with this condition[3].

Certain studies have confirmed that the functional changes of abnormal immune cells could induce damage and inflammation in the glomerular area, which can also lead to tissue loss[4]. Among these abnormal immune cells, macrophages played an important role in LN [5] and these are formed by the mature differentiation of monocytes which can recognize, engulf and destroy target cells, and they play a vital role in regulating the inflammatory response and host defense. Monocytes can differentiate into two types of macrophages with different phenotypes and functions after receiving different external stimulations.

There are two classical types of macrophages are M1-phenotype macrophages with pro-inflammatory effects and M2-phenotypes with immunosuppressive effects [6]. M1 type macrophages are characterized by an enhanced ability to secrete pro-inflammatory factors such as interleukin − 1β (IL-1β), tumor necrosis factor (TNF), interleukin-12 (IL-12) and interleukin-18 (IL-18), as well as antigen-presentation and initiating the adaptive immune response. The high expression levels of major histocompatibility complex type II molecules (MHC-II), CD68, CD80 and CD86 markers, and inducible nitric oxide synthase (iNOS) are specific characterizations of M1 type macrophages. In addition, the up-regulation of CD200R membrane glycoprotein and CD163-CMAF are distinct markers of M2 type macrophages[7]. M2 type macrophages can secrete anti-inflammatory factors such as IL-10, transforming growth factor-β (TGF-β) and up-regulate the expression of arginase-1 (Arg-1), which exhibit obviously anti-inflammatory effects for immune response suppression[8]. The imbalance of M1/M2 macrophages and cytokines are collectively involved in the progression of LN. Despite the dominant effect of macrophages in LN, there is currently no consistent data as their precise role in this disease.

Fractalkine (FKN, CX3CL1) is a cell chemokine encoded by the *CX3CL1* gene. FKN is mainly expressed in endothelial cells. T cells and monocytes can be attracted by the soluble form of FKN (sFKN), and can further to promote the adhesion of monocytes to activated endothelial cells[9]. Studies have shown that the monocyte-endothelial cell adhesion effect mediated by the FKN-CX3CR1 interaction promotes the progression of a variety of inflammatory and autoimmune diseases including LN[10]. Our research group has confirmed that the expression levels of FKN were positively correlated with the severity of LN and higher FKN levels in patients can trigger this condition and cause the kidney injury. The expression levels of FKN were also positively correlated with SLEDAI-2K, and were negatively correlated with the complement proteins, C3 and C4, in LN patients[11]. In addition, FKN was associated with the presence of autoantibodies, indicating the potential of FKN in mediating the pathogenesis in LN. However, the specific mechanism of this is still unclear.

The Hippo pathway is an evolutionarily conserved signaling pathway that regulates cell growth, fate decisions as well as control of organ size and regeneration. Such multiple functions are widely conserved among species and cell types[12]. The main intracellular effectors of this signaling cascade are mammalian Ste20-like kinases 1/2 (MST1/2), large tumor suppressor 1/2 (LATS1/2), yes-associated protein (YAP) and the paralog transcriptional coactivator with PDZ-binding motif (TAZ). When this signaling cascade is activated, MST1/2 proteins phosphorylate and activate LATS1/2 factors which in turn phosphorylate YAP/TAZ factors, resulting in the inhibition of YAP/TAZ transcriptional activity.

However, YAP and TAZ can also translocate into the nucleus to serve as co-transcriptional factors when Hippo pathway is not activated[13]. Numerous studies have found that the Hippo signaling pathway plays a key role in both innate and adaptive immune responses. Similarly, there have been recent reports in mice models and humans to confirmed the abnormal expression of Hippo pathway members in cancer and a variety of auto-immune disease (AID), such as rheumatoid arthritis (RA), SLE, and Sjögren's syndrome (SS)[14, 15]. However, the potential mechanisms through which the Hippo signaling pathway interacts with FKN in LN have not been reported. Studies of its molecular mechanism may provide a new insight for clarifying the molecular mechanism of FKN in regulating the development of inflammatory diseases.

We first found an abnormal expression of Hippo signaling pathway in patients with LN, and this was related to the severity of LN and kidney damage. Furthermore, by using INF-γ-induced macrophages and constructing FKN knockout LN mouse models, it was confirmed that FKN could mediate an imbalance in INF-γ-induced macrophage polarization through the Hippo signaling pathway. FKN deficiency could activate the Hippo signaling pathway and reduce the activation of macrophages and this was further confirmed in the LN mouse model. This was also shown to reduce the renal damage caused by LN.

Materials And Methods

Clinic data collection

The study was approved by the Affiliated Hospital Ethics Committee of Youjiang Medical University for Nationalities (Baise, Guangxi Province, P.R. China) and informed consent was obtained from all participants. 91 newly diagnosed patients with LN and 64 healthy controls were selected in this study. All participants were initially diagnosed with LN from May 2019 to May 2021 at the Affiliated Hospital of Youjiang Medical University for Nationalities. Patients with LN were aged 42±16 years with mean proteinuria of 7.9±1.4g/24h and a mean estimated GFR of 69±20mL/min/1.73m^2 . SLE was diagnosed according to the revised criteria of the American Rheumatism Association in 1997. Patients were clinically diagnosed as LN by kidney biopsies according to the International Society of Nephrology (ISN)/Renal Pathology Society classification[11].

All patients with LN were divided into two subgroups as active LN (score≥10) and inactive LN (score<10) according to SLEDAI-2K or for LN with renal damage (GFR< 60ml/min) and without renal damage (GFR≥60ml/min) according to patients' renal function. The definition of leukopenia was that the white blood cell count was <3.5 ×10 9 /L. The definition of anemia was that the hemoglobin was <110g/L for female (<120g/L for male). The definition of thrombocytopenia was that the blood platelet count was <100×10^9/L. Patients with C-reactive protein (CRP) of more than 3mg/L were defined as elevated. Serum complement of C3 <580mg/L and complement of C4 < 70mg/L were regarded as decreasedAll patients have signed the informed consent forms. Laboratory test results (including routine blood tests, GFR, C3, C4, anti-Sm antibody) were collected before treatment. Peripheral blood was collected from patients with LN before they received any immunosuppressive treatment which included glucocorticoid and an

immunosuppressant[11]. An aliquot of the collected fresh blood sample was used for PCR, and the serum was extracted in the rest of the samples and stored at -80°C for later use.

Cell culture

RAW264.7 cells were obtained from the Beina Chuanglian Biology Research Institute (BNCC300973, Beijing, China). Cells were cultured in DMEM (Gibco) with 10% fetal bovine serum (Gibco) at 37°C in a 5% CO_2 incubator. RAW264.7 cells were infected with lentiviral vector particle-CX3CL1 and Ubi-MCS-3FLAG-SV40-Cherry-IRES-negative control according to manufacturer's protocol (Shanghai GeneChem Co., Ltd.) to achieve FKN overexpression. RAW264.7 cells were infected with lentiviral vector particle-CX3CL1 and hU6-MCS-CBh-gcGFP-IRES-negative control according to manufacturer's protocol (Shanghai GeneChem Co., Ltd.) to achieve FKN knockdown. Stable cell lines were selected by adding puromycin in the culture medium[16]. Cells were divided into 12 groups as follows:

1. control group with no treatment
2. IFN-γ group: cells were infected with IFN-γ (Peprotech, Cranbury, NJ, USA) (the IC_{50} for RAW264.7 cells was 400ng/mL) 400ng/mL for 48 hours
3. VP (Hippo signaling pathway inhibitor) group: cells were infected with Verteporfin (HY-B0146 MCE, MedChemExpress, NJ, USA) (the IC_{50} for RAW264.7 cells was 2uM) 2uM for 48 hours
4. IFN-γ+VP group: cells were treated with 400ng/mL IFN-γ and 2uM VP for 48 hours
5. Ex-FKN group
6. Ex-FKN+IFN-γ group: ex-FKN cells infected with 400ng/mL IFN-γ for 48 hours
7. Ex-FKN+VP group: ex-FKN cells infected with 2uM VP for 48 hours
8. Ex-FKN+IFN-γ+VP group: ex-FKN cells were treated with 400ng/mL IFN-γ and 2uM VP for 48 hours
9. Si-FKN group
10. Si-FKN+IFN-γgroup: si-FKN cells infected with 400ng/mL IFN-γ for 48 hours
11. Si-FKN+VP group：si-FKN cells were infected with 2uM VP for 48 hours
12. Si-FKN+IFN-γ+VP group: si-FKN cells were treated with 400ng/mL IFN-γ and 2uM VP for 48 hour.

Mice

2-3-month-old (22-28g) specific pathogen- free (SPF) WT C57BL/6 mice ($FKN^{+/+}$) and KO-FKN C57BL/6 mice ($FKN^{-/-}$) were purchased from Shanghai Genechem Animal Co. Ltd (NO.SYXK 2015-0008). For KO-FKN mice, CRISPR/Cas9 technology was used to construct an sgRNA sequence (CX3CL1-sgRNA1:CTGGCAGGTTATCACGGGTTGGG;CX3CL1-sgRNA2:TGGCAGTAACTCATACGTCCTGG) that targeted the FKN gene locus. The surviving embryos after injection with CRISPR/Cas9 mRNA were raised to adulthood, and then the founders with FKN knockout were selected. Before the experiment, mice were maintained in a room with controlled temperature (23 ± 1℃), humidity and lighting (12-h light/12-h dark cycle), and given free access to food and water[16]. The animal experiment protocol was approved by the

animal experiment ethics of Youjiang Medical University for Nationalities and carried out in compliance with the Animals in Research: Reporting In vivo Experiments (ARRIVE) guidelines. All animal procedures were in accordance with the Guide for the Care and Use of Laboratory Animals (NIH Publication No. 85–23, revised 1996).

8-10 weeks old WT and KO-FKN ($FKN^{-/-}$) female mice were selected, and an LN mouse model was induced by a single intraperitoneal injection of 0.5mL pristane (P815856, Shanghai Macklin Biochemical Co., Ltd). When constructing the model, different parameters including the mouse body weight, joint diameter and urine protein concentration as well as the anti-ANA, anti-Sm and anti-dsDNA antibody concentration were measured every 4 weeks. The LN models of WT and $FKN^{-/-}$ mice were established approximately 4-6 months later. Subsequently, the mice were randomly divided into 8 groups with 3-5 animals in each group):

1. WT group: WT mice were intraperitoneally injected with 500uL of normal saline every day for 10 consecutive days
2. WT+VP group: VP was dissolved in dimethyl sulfoxide (DMSO, 0.05% v/v), and DMSO (0.05%v/v) was used as the vehicle. WT mice were intraperitoneally injected with VP (100mg/kg) daily for 10 days.
3. LN group: LN mice were intraperitoneally injected with 500uL of normal saline every day for 10 consecutive days.
4. LN+VP group: LN mice were intraperitoneally injected with VP (100mg/kg) daily for 10 days
5. KO-FKNgroup: KO-FKN mice were intraperitoneally injected with 500uL of normal saline every day for 10 consecutive days
6. KO-FKN+VP group: KO-FKN mice were intraperitoneally injected with VP (100mg/kg) daily for 10 days
7. KO-$FKN^{-/-}$+LN group: KO-FKN mice with LN were intraperitoneally injected with 500uL of normal saline every day for 10 consecutive days
8. KO-FKN+LN+VP group: KO-FKN mice with LN were intraperitoneally injected with VP (100mg/kg) daily for 10 days.

Then, the mice were sacrificed after the last injection 10 days later. The animals were weighed and anaesthetized with 1% pentobarbital (35 ml/kg i.p.), and kidney samples were collected for histological examination and immunofluorescence staining. Some samples were also stored at -80℃ for analysis by western blotting.Great efforts were made to minimize the pain of animals.

ELISA

The collected serum was used for ELISAs. The following ELISA kits were purchased including YAP (JL45328, Shanghai Jianglai Co. Ltd.), TAZ (JL19183, Shanghai Jianglai Co. Ltd.), MST (CSB-E09062h, Cusabio Biotech Co. Ltd), IL-6 (CSB-E04638h, Cusabio Biotech Co. Ltd.) and IL-10 (CSB-E04593h, Cusabio

Biotech Co. Ltd.) and used according to the manufacturers' instructions. A TriStar LB941 multimode microplate reader was used to measure the absorbance at 450 nm.

Renal function measurements

Metabolic cages (Nalgene, Rochester) were used to collect mice urine samples for a 24-hour period. Urinary protein collected over 24 hours was measured using a urine protein assay kit (C035-2-1, Jiancheng Bioengineering Institute) according to the manufacturer's instructions. The stored mouse serum was used to measure blood urea nitrogen (BUN) and serum creatinine (Scr) in order to assess renal function. A BUN assay kit (C013-2-1, Jiancheng Bioengineering Institute) and a creatinine assay kit (C011-2-1, Jiancheng Bioengineering Institute) were respectively used to measure the serum levels of Scr and BUN of mice according to the manufacturer's instructions.

Cells viability assay

A cell counting kit (M4839, AbMole, Beijing, China) was used to assess the viability of cells. RAW264.7 cells were seeded into 96-well plates at 5×10^3 cells per well and then treated with different concentrations of IFN-γ (100, 200, 300 and 400 ng/mL) and VP (0, 0.5, 1and 2 μM) for 24, 48 and 72 hours. 10 μL CCK-8 was added to each well and incubated for 1 hour at 37°C in an incubator in an atmosphere of 5% CO_2 after the treatment with IFN-γ and VP. The OD was measured using a TriStar LB 941 multimode microplate reader (Berthold Technologies, Germany) at 450 nm.

Cell apoptosis assay

The fluorescein isothiocyanate-annexin V/propidium iodide (FITC-annexin V/PI) apoptosis kit (556 547, BD Biosciences) was used to assess cell apoptosis. Cells in different groups were cultured for 48 hours, collected, washed twice with PBS buffer, and buffer was added to adjust the RAW264.7 cell concentration to $1x10^5$ cells/mL. 5 μL of FITC-annexin V/PI was added, then incubated for 15min at room temperature in the dark. The apoptosis rate was measured within 1 hour after adding 400 μL of buffer by flow cytometry.

HE, PASM and Masson staining

Kidney tissue samples were fixed in 10% formalin and then embedded in paraffin for histopathology. 3-4 μm serial sections dewaxed and hydrated and then stained with haematoxylin-imidine red (HE), Masson and periodic acid-silver methenamine (PASM) stains according to standard procedures. These sections were subsequently visualized using a light microscope (Nikon Eclipse E100).

Immunofluorescence assay

RAW.267.4 cells (5×10^3 cells/well) were seeded into glass bottom cell culture dishes (IBIDI, Germany) for 72 hours. After the slides were dried slightly, 50-100μL of a rupture working solution was added, incubated at room temperature for 20min and washed 3 x 5min with PBS. Then 3% BSA was added to

cover the tissue section evenly, and then these were sealed at room temperature for 30 minutes. Cells were incubated with fluorescently labelled primary antibodies (anti-FKN, anti-p-YAP, anti-IL-10 or anti-TNF-a) followed by either goat anti-rabbit IgG (H + L) FITC-conjugated antibody (S0008, 1:200, Affinity) or goat anti-mouse IgG (H + L) Fluor594-conjugated antibody (S0005, 1:200, Affinity). Finally, cells were incubated with DAPI for 10 minutes and imaged using an Olympus Fluoview 3000 Confocal Laser Scanning Microscope (FV3000, Olympus and Tokyo) the cells and collect the images[16].

Mice kidney sections were prepared according to standard procedures. The primary antibodies used included anti-F4/80, anti-p-YAP, anti-IL-10 and anti-TNF-a followed by secondary antibody staining as described above for cells. An Olympus Fluoview 3000 Confocal Laser Scanning Microscope was used as described above.

Western blotting

50ug total protein extracts were separated by SDS-polyacrylamide gel electrophoresis (SDS-PAGE) and transferred to PVDF transfer membranes (Thermo Scientific, Illkirch, France). The membranes were incubated overnight at 4°C with different antibodies. The primary antibodies used for western blotting were rabbit anti-FKN(DF12376,1:1000, Affinity), rabbit anti-iNOS(AF0199, 1:1000, Affinity), rabbit anti-YAP (DF3182, 1:1000, Affinity), rabbit anti-phospho-YAP (AF3328, 1:1000, Affinity), rabbit anti-TAZ (DF4653, 1:1000, Affinity), rabbit anti-phospho-TAZ (AF4316, 1:1000, Affinity), rabbit anti-TNF-α (AF7014, 1:1000, Affinity), rabbit anti-IL-10 (DF6894, 1:1000, Affinity), anti-Arg-1 (DF6657, 1:1000, Affinity), rabbit monoclonal FKN antibody (ab25091, 1:1000, Abcam), rabbit anti-iNOS (18985 1:1000, Proteintech), rabbit anti-MST1 (3682, 1:3000, CST) and rabbit anti-MST (DF8430, 1:1000, Affinity). The membranes were then incubated with either goat anti-rabbit IgG (S0001,1:5000,Affinity) or goat anti-mouse IgG (S0002, 1:5000, Affinity) for 60 minutes at room temperature, then exposed to an enhanced chemiluminescence substrate (KF003, Affinity) and visualized using a Tanon-5200 (Tanon, Shanghai, China)[16].

Preparation of PBMCs and RT-qPCR

Five milliliters of peripheral blood were collected in evacuated tubes containing EDTA as the anticoagulant. PBMCs were purified from peripheral blood by centrifugation. The One-step Trizol-based procedure was used for total RNA extraction from freshly isolated PBMCs. RNA was reverse transcribed into cDNA after the purity and concentration was checked. The YAP primer sequence was: forward primer 5'-GCTTCCCCGACTACCTG-3', reverse primer 5'- CACAGACTCCACGTCCAA-3' with a product size of 146bp. The MST1 primer sequence was: forward primer 5'-GCAGTGTGCGTTTCCAGA-3', reverse primer 5'-CAGGTCCCAGCGTTGAC-3' with a product size of 131bp. The TAZ primer sequence was: forward primer 5'-AGGGAGGGAACAGAGCA-3', reverse primer 5'-GTGAGCAGTGGGCAAGTAG-3' with a product size of 123bp. The internal reference GAPDH primer sequence was: forward primer 5'-CAGGAGGCATTGCTGATGAT-3', reverse primer 5'-GAAGGCTGGGGCTCAGGG-3' with a product size of 84bp. The PCR reaction system consisted of a SYBR Green Mix, forward and reverse primers, cDNA and deionized RNAase-free water. The PCR was initially denatured at 95 °C for 30s followed by 95°C for 10s and 65°C for 30s for 40 cycles and 81 cycles at 55-95°C for 10 s for the melting curve analysis. After the

cycle threshold (Ct) was determined, the expression of YAP,TAZ and MST1 mRNA was quantified according to the reference gene and analyzed by using the $2^{-\triangle\triangle Ct}$ method[16].

Statistical analysis

Histograms and data are shown as mean±SD of a minimum of three independent experiments. SPSS 23.0 and GraphPad Prism 8.0 were used to analyze all statistical data. $P<0.5$ was considered to be statistically significant.

Results

The expression of Hippo signaling pathway in PBMCs isolated from LN patients

Compared with the control group, the serum expression levels of YAP and TAZ in the inactive and active LN groups were significantly increased (P 0.01), while the expression level of MST1 decreased (P 0.01). The levels of YAP and TAZ in the active LN group were higher than those in the inactive LN group (P 0.05), and the MST1 expression level was lower than that in the inactive LN group (P 0.05) (Fig. 1A). Compared with the control group, the peripheral blood YAP and TAZ mRNA expression levels in the inactive LN and active LN groups were dramatically increased (P 0.01), while the MST1 mRNA expression levels in active LN was decreased compared with healthy controls (P 0.01). The levels of YAP and TAZ mRNA in the active LN group were higher than those in the inactive LN group (P 0.05), and the MST1 mRNA expression levels was not different between the two groups (Fig.1B).

The relationship between the Hippo signaling pathway and disease activity in LN patients

Serum YAP and TAZ levels were positively correlated with the disease activity of LN patients. The Hippo-YAP/TAZ serum levels were positively correlated with SLEDAI-2K in LN patients (r=0.284, p=0.006; r=0.464, p=0.000) (Figs. 1C, 1D). These results suggested that the high YAP and TAZ expression levels were accompanied by an increased SLADAI-2K score so as to result in aggravation of the disease.

The relationship between the Hippo signaling pathway and renal damage in LN patients

When compared to the control group, the serum expression levels of YAP and TAZ in the LN patients without renal damage and those with renal damage were significantly increased (P 0.01), while the expression level of MST1 decreased (P 0.01). The expression levels of YAP and TAZ in the LN patients with renal damage were higher than those LN patients without renal damage (P 0.05), and the MST1 expression level was not different between these two groups (Fig.1E). The serum YAP level was inversely proportional to the GFR of LN patients (r=0.-0.213, p=0.042). The higher the YAP level, the lower the GFR and the more serious the renal damage seen. Serum TAZ and MST1 levels were not correlated with GFR (Fig.1F).

Associations of the Hippo signaling pathway with laboratory parameters of LN patients

The associations of the Hippo signaling pathway with other clinical laboratory parameters of LN patients are shown in Table 1. Serum TAZ concentrations were negatively correlated with those of complement C4. It was found the higher the TAZ expression level, the lower the complement C4 expression level. The expression levels of YAP and TAZ were also correlated with the expression levels of anti-dsDNA and anti-Sm. The expression levels of YAP and TAZ in ds-DNA positive patients were significantly increased (Table 1).

Table 1

Associationsbetween serum levels of YAP,TAZ and MST1andthe laboratory parameters of LN patients.

Group	+/-	Number of patients	Serum YAP levels(ng/mL)	Serum TAZ levels(ng/mL)	Serum MST1 levels(ng/mL)
Leukopenia	-	65	4.32±0.46	9.55±1.06	21.39±2.32
	+	26	4.33±0.50	9.62±0.79	21.20±2.50
Thrombocytopenia	-	76	4.32±0.47	9.63±0.82	21.48±2.47
	+	15	4.31±0.49	9.62±0.69	20.56±1.44
Anemia	-	25	4.26±0.54	9.42±0.68	21.53±2.05
	+	66	4.34±0.44	9.71±0.82	21.27±2.48
CRP elevated	-	30	4.30±0.48	9.46±0.66	21.21±1.94
	+	61	4.33±0.46	9.71±0.85	21.40±2.55
C3 decreased	-	51	4.26±0.48	9.56±0.83	21.37±2.23
	+	40	4.40±0.44	9.72±0.75	21.29±2.54
C4 decreased	-	49	4.30±0.47	9.45±0.82[a]	21.49±2.64
	+	42	4.34±0.47	9.84±0.72	21.15±2.00
Anti-dsDNA	-	47	4.16±0.44[b]	9.21±0.64[b]	20.94±2.43
	+	44	4.49±0.44	10.07±0.71	21.70±2.25
Anti-Sm	-	64	4.25±0.49[c]	9.49±0.77[c]	21.40±2.15
	+	27	4.48±0.48	9.95±0.77	21.31±2.46

[a]Compared to LN without a decrease in C4 levels,p<0.05.

[b]Compared to LN with anti-dsDNA positivity,p<0.05.

[c]Compared to LN with anti-Sm positivity,p<0.06.

FKN promoted the apoptosis of IFN-γ-induced macrophages via the Hippo signaling pathway

As shown in Figure 2, compared with the control group (26.3±0.10), the apoptosis rate of the IFN-γ (38.9±0.1), VP (62.5±27.5), IFN-γ+VP (91.5±8.61), ex-FKN+VP (47.06±21.81), ex-FKN+IFN-γ+VP (79.93±21.61), si-FKN (56.40±1.00), si-FKN+IFN-γ (69.60±0.53), si-FKN+VP (91.93± 3.75) and si-FKN+IFN-γ+VP (98.66±0.35) groups were all increased markedly (P<0.01). The apoptotic rates of the ex-FKN

(0.03±0.01) and ex-FKN+IFN-γ (0.04±0.03) groups were lower than that of the control group (P<0.01), which indicated that these three intervention factors (IFN-γ as well as knocking down FKN and VP) could all promote the apoptosis of RAW264.7 cells. Conversely, the overexpression of FKN could inhibit the apoptosis of RAW264.7 cells. In addition, compared with the IFN-γ group (38.9±0.1), the ex-FKN+IFN-γ group (0.04±0.03) had a decreased apoptotic rate (P<0.01), whereas the rate was increased in the si-FKN+IFN-γ group (69.60±0.53; P<0.01).

FKN negatively regulated the Hippo signaling pathway and promoted the polarization of IFN-γ-induced RAW264.7 macrophages towards the M2 phenotype

Western blotting and immunofluorescence (IF) analysis were used to assess the expression of the component of the Hippo signaling pathway target protein in each group. Compared with the control group, when FKN was overexpressed, the expression of YAP was increased, and the expression of MST1, p-YAP and p-TAZ were conversely decreased. When FKN was knocked down, the expression of YAP decreased, while the expression of MST1, p-YAP and p-TAZ were all up-regulated (p<0.05). In addition, under the influence of IFN-γ, the expression of YAP was further enhanced, and the expression levels of MST1, p-YAP and p-TAZ were further reduced (p<0.05; Figs. 3A-B, 3D-E). Together these results suggested that both IFN-γ and FKN could inhibit the Hippo signaling pathway, while FKN knockdown could activate this pathway. Through IF staining, it was observed that p-YAP protein accumulated in cytoplasm. Overexpression of FKN could increase the expression of YAP, and down-regulate the expression of p-YAP, therefore the presence of the phosphorylated form in the cytoplasm was reduced. Moreover, the Hippo pathway was inhibited by overexpression of FKN, and IFN-γ further enhanced this inhibitory effect. However, the localization of p-YAP into the cytoplasm was facilitated after the knockdown of FKN and the intervention of VP treatments could reverse this inhibitory effect (Fig.3E). Overall, these results revealed that FKN and Hippo signaling pathways interacted in an opposing way in IFN-γ-induced RAW264.7 macrophages.

The expression levels of iNOS, TNF-α, IL-10 and Arg-1 in each group was also measured by using western blotting and IF in order to investigate the driving force of FKN on the polarization process of IFN-γ-induced RAW264.7 cells. Figures 3A and 3C show that the expression of the macrophage polarization cytokines of iNOS, TNFα, IL- 10 and Arg-1 in the FKN overexpression group were increased when compared with control group (P<0.05). In addition, macrophage polarization was highly enhanced after IFN-γ treatment (P<0.05). This also confirmed the macrophage polarization process was induced by IFN-γ. Furthermore, when FKN was knocked down, the expression levels of IL-10, Arg-1, iNOS and TNF-α were also decreased, with almost no expression of the M2 type macrophage polarization-related factors IL-10 and Arg-1. The RAW264.7 cells expressed mainly the M1 type polarization factors, iNOS and TNF-α, and the macrophage balance was biased towards the M1 phenotype.

A combined treatment with VP significantly weakened the effects of FKN on the cells. Through IF staining, the expression levels of IL-10 and TNF-α proteins were observed in both the nuclei and cytoplasm but they were mainly located in the latter after IFN-γ stimulation when compared with the

controls. FKN overexpression could enhance the localization of IL-10 and TNF-α while FKN knockdown could decrease their localization in IFN-γ-induced RAW264.7 cells. However, the decreasing trend of IL-10 was more obvious than that seen for TNF-α. VP reversed the effects of FKN (Figs. 3F-3G).

Taken together, all the above results indicated that FKN overexpression could inhibit the activation of the Hippo signaling pathway, reduce the phosphorylation levels of the components in Hippo signaling pathway and increase the activation of macrophages. After FKN knockdown, the Hippo signaling pathway was activated, and the phosphorylation levels of its related proteins were increased. In addition, the level of macrophage activation was decreased and the polarization imbalance of macrophages was biased toward M1 phenotype.

FKN deficiency can reduce the polarization and proliferation of macrophages in LN by activating the Hippo signaling pathway, thereby reducing renal damage

Using LN-induced mice, we further studied whether FKN deficiency could affect the proliferation and polarization of macrophages through the Hippo signaling pathway, thereby reducing the observed related kidney damage. FKN deficient (KO-FKN) mice were used and Scr, BUN and 24 hour urinary protein were measured as markers of renal function. As shown in Figure 4A, the levels of these three parameters were markedly reduced in the KO-FKN+LN when compared with the WT+LN mice (P<0.05). The above indicators were further reduced in VP-treated mice (P<0.05) (the KO-FKN+LN+VP group). These findings were further supported by the pathological alterations seen in HE-, Masson- and PASM-stained mice kidney tissues. The sub-cellular structures in the kidney tissues in the LN group were severely abnormal, with a large number of inflammatory cell infiltration in the interstitium, as indicated by the red arrows (Fig. 4B). In addition, abscesses and a large number of necrotic neutrophils were seen in the lumen of some renal tubules, as shown by the yellow arrows (Fig. 4B). A large number of tubules were dilated and parts of the protein deposits can be seen as shown by the black arrows (Fig. 4B). The glomerulus cavities were also dilated. However, when FKN was deficient or the animals were treated with VP, these renal structural changes in the LN group largely were alleviated. As shown in Figure 4B, the kidney damage in the KO-FKN+LN+VP group was decreased.

Western blot analysis was used to measure the protein expression levels of FKN, MST1, YAP, p-YAP, p-TAZ, iNOS, TNF-α, IL-10 and Arg-1. LN mice in the FKN deficient (KO-FKN+LN) group showed decreased protein expression of FKN, YAP, iNOS, TNF-α, IL-10 and Arg-1compared with the WT+LN group (P<0.05), while the expression levels of MST1, p-YAP and p-TAZ were increased (P<0.05). When combined the treatment of VP (the KO-FKN+LN+VP group) this further inhibited the expression of FKN, YAP, iNOS, TNF-α, IL-10 and Arg-1, thus strengthening the effect of FKN deficiency (P<0.05; Figs.5 A-B).

Kidney tissues were also stained with antibodies to F4/80, p-YAP, IL-10 and TNF-α in order to identify macrophage accumulation and progress of polarization. When compared with WT mice, the localization of F4/80, IL-10 and TNF-α proteins in the kidneys of LN mice was enhanced, while p-YAP localization was decreased. Furthermore, F4/80, IL-10 and TNF-α proteins localized in mice kidney tissues were markedly reduced in the KO-FKN+LN and KO-FKN+LN+VP groups when compared with the LN group, while the

expression of p-YAP was increased (Figs. 5C-5E). These results were consistent with the Western blotting assays. Taken together, these data showed that FKN deficiency could activate the Hippo signaling pathway, and increase the phosphorylation of proteins such as YAP and TAZ as well as reducing the activation of macrophages in LN, thereby relieving the associated renal damage.

Discussion

SLE is a classic systemic autoimmune disease, with the involvement multiple organs and a variety of autoantibodies as the main clinical features[17]. LN is a disease in which SLE involves the kidneys and causes different pathological types of immune damage accompanied by a series of complications such as proteinuria, hematuria and anemia.10 to 30% of LN patients will develop renal failure, which is the main cause of death in SLE patients[18]. Our previous study found that there was a correlation between the expression level of FKN and the degree of renal damage and disease activity in LN patients. In this study, we further demonstrated that inhibition of the Hippo signaling pathway in LN patients was related to the disease activity and renal damage in LN patients. Knockout of FKN could activate the Hippo signaling pathway and increase the phosphorylation of proteins such as YAP and TAZ, thereby reducing the infiltration and activation of kidney macrophages and limit the accompanied LN kidney damage.

There is an imbalance of M1/M2 macrophages in LN. Macrophages and their secreted cytokines play a mixed role. As a kidney infiltrating cell, the number of macrophages increases with the progression of kidney injury, and it is closely related to the patient's proteinuria and activated deposit levels[19]. Moreover, activated macrophages continue to proliferate in the kidney tissue and participate in the formation of crescents in the kidneys of patients with LN[20]. Some researchers have shown that M1 macrophages mainly played a role in promoting inflammation and fibrosis, while the M2 macrophages were capable of an anti-inflammatory effect and could promote the repair and reconstruction process of damaged tissues[21]. Depletion of M1 type macrophages, suppression of their recruitment and destruction of inflammatory macrophages polarization could significantly improve nephritis in mice with several different LN models[22]. Other studies have suggested that the kidney damage that occurs as a result of LN was related to the infiltration of M1 macrophages and lymphocytes. M1 macrophages secrete IFN-γ, which could act as an inflammatory factor to up-regulate the inflammatory immune response and promote the recruitment of more macrophages[23]. The M1 type of macrophages in LN express the pro-inflammatory factor, MCP-1, strongly. When the MCP-1 gene was knocked out or an inhibitor was used to block MCP-1 or its receptor, this could reduce their infiltration, thereby reducing the inflammation reaction[24]. However, other researchers pointed out that the kidney tissue of patients with LN was mainly infiltrated with M2 type macrophages. When activated, these macrophages expressed CD163 and they were the most abundant macrophage subtype in kidney biopsy of patients with LN. CD163 could even be used as a biomarker of LN disease activity[25]. The question as to which type of macrophages are dominant in LN is still open to debate as the current research results are not consistent.

FKN is the only known member of the CX3C family. After binding to its unique receptor, CX3CR1, it can be used as a transport medium to mediate the migration of macrophages, lymphocytes, dentritic cells (DCs)

and natural killer (NK) cells, and promote their antigen presentation, phagocytosis and immune regulation[26]. FKN plays an important role in inflammation due to its unique functions and structural characteristics[27], and it participates in the pathogenesis of various diseases including acute necrotizing pancreatitis, uveitis, neuropathic pain and rheumatoid arthritis[28, 29]. In recent years, studies have shown that FKN was closely related to kidney disease. *In vivo* experiments have found that FKN could regulate renal interstitial fibrosis in a mouse model of ischemia-reperfusion injury through its cognative receptor, CX3CR1[30]. Another reports pointed out that FKN might be related to the interstitial lesions of human crescentic glomerulonephritis before corticosteroid treatment[31].

In this study, FKN was shown to promote the apoptosis of RAW264.7 cells induced by IFN-γ. When FKN was overexpressed, the secretion of IL-10, Arg-1, iNOS and TNF-α were further enhanced. When FKN was knocked down, the secretion of IL-10, Arg-1, iNOS and TNF-α were all reduced, but the decrease of IL-10 and Arg-1 of the M2 type macrophage polarization index was greater than that of iNOS and TNF-α, which were the M1 type macrophage polarization indicators. Thus, the polarization imbalance of macrophages was biased towards M1 type. Moreover, overexpression of FKN led to an increase in the expression of YAP and decreases in the levels of MST, p-YAP and p-TAZ. This indicated that overexpression of FKN could inhibit the Hippo signaling pathway and reduce the phosphorylation of its related proteins.

IFN-γ-induced RAW264.7 also showed increased macrophage activation. When FKN was knocked down, the expression of YAP was decreased, and the expression levels of MST, p-YAP and p-TAZ were increased, indicating that the Hippo signaling pathway was activated. A similar result was found in FKN-deficient LN mice, where the expression of YAP in the Hippo signaling pathway was decreased as well as the expression levels of iNOS, TNF-α, IL-10 and Arg-1. Kidney pathological and immunofluorescence results suggested that the kidney damage of FKN gene knockout mice was significantly reduced. This indicated that the Hippo signaling pathway was activated after FKN knockout, the phosphorylation levels of YAP and TAZ were increased, the activation of renal macrophages was reduced and the polarization of M1/M2 was biased toward the M1 direction. This subsequently reduced glomerular atrophy, glomerular basement membrane proliferation and inflammatory cell infiltration, thereby improving the associated kidney injury.

The Hippo signaling pathway is a highly conserved kinase cascade, which consists of three parts: upstream regulatory factors, a core kinase complex and a downstream transcriptional regulatory complex. Under normal circumstances, MST1/2 kinase binds to the regulatory protein, Sav1, phosphorylates and activates LATS1/2. At the same time, activated LATS1/2 binds to the regulatory protein Mob1 to phosphorylate the downstream effector molecules YAP/TAZ. When phosphorylated, these proteins lose their transcriptional activities, remain in the cytoplasm, and are degraded through different pathways, thereby inhibiting proliferation, promoting apoptosis and maintaining the steady state of tissue cell growth[32]. Under pathological conditions, the Hippo signaling pathway is blocked or inhibited. YAP and TAZ are activated by dephosphorylation, which promotes nuclear metastasis and combines with transcription factors such as TEAD to promote proliferation and mediate the development of various diseases[33].

Recent studies have shown that the Hippo pathway is involved in a wide range of cellular processes including programmed cell death, regulation of mitochondrial homeostasis, participation in damage repair, mediating the progression of organ fibrosis and playing an important role in the pathogenesis of kidney injury. Feng et al. [34]revealed in more detail the causal relationship between MST1 activation and acute kidney injury (AKI). This study showed that the up-regulation of MST1 was a key step in causing renal ischemia and reperfusion (IR) injury. An increase in MST1 could induce mitochondrial division by blocking the AMPK-YAP pathway, promoting renal tubular epithelial cell apoptosis and aggravating the inflammatory response and renal function damage. In this study, however, we found that the expression level of MST1 in LN patients was decreased and it was negatively correlated with renal damage. Its expression was also low in LN mice, which were not consistent with the above research results. However, the results of Feng's study were from using the AKI model. After all, LN causes renal damage in a chronic and continuous process. Therefore, whether MST1 also induces mitochondrial division during this process and inhibits mitochondrial autophagy in order to cause renal damage remains to be further studied. Similarly, the Hippo signaling pathway regulates the YAP signaling axis and is closely related to the de-differentiation, migration and proliferation of renal tubular epithelial cells.

Xu’s [35]reported that the Hippo signaling pathway had both a beneficial effect as well as an adverse effect on the kidneys. When the kidney tissues suffered from only mild to moderate damage, YAP transiently increased in the cytoplasm and nucleus, and this promoted the complete regeneration and repair of the kidney tissue. However, when the damage was severe, the expression levels of YAP and the downstream proteins would continue to increase and become activated, thereby mediating the process of renal fibrosis. It was suggested that the transient increasing of YAP might induce the remnant tubular epithelial cells to transform from a mature quiescent to a proliferative state, thereby exerting renal protection. In addition, the continuous activation of YAP might inhibit the re-differentiation of poorly regenerated tubular epithelial cells, and then have adverse effects on kidneys. Our results showed that in LN patients and LN mice, YAP expression was increased and may be continuously activated, while the expression levels of p-YAP and p-TAZ were decreased, indicating that the HippoYAP signaling pathway was inhibited. YAP and TAZ are activated when dephosphorylated, which promote nuclear metastasis and proliferation. This inhibits the re-differentiation of poorly regenerated tubular epithelial cells, which ultimately leads to the damage of renal function. On the other hand, there were also studies that showed that the Hippo signaling pathway was closely related to autoimmune diseases[36]. However, the relationship between Hippo signaling pathway and LN has been rarely reported. YAP activation recruits and activates macrophages, protecting tumor cells from lymphocyte-mediated immune surveillance in the tumor model[37].

Our results also showed that the levels of YAP and TAZ in peripheral blood of LN patients were increased, and were positively correlated with LN disease activity and renal damage. This indicates that LN not only increased the expression of FKN, but also inhibited the Hippo signaling pathway. Further cell experiments showed that the expression of YAP increased and the Hippo signaling pathway was inhibited when FKN was overexpressed, which eventually led to macrophage activation and an imbalance in their polarization. After knocking down FKN, the results were opposite, and the results of animal experiments

were consistent with this. The expression of YAP in knockout mice with LN was decreased, and the Hippo signaling pathway was activated. Eventually, the infiltration and activity of kidney macrophages decreased, and the extent of renal function damage was reduced. This further showed that under the control of FKN, the Hippo signaling pathway could act on macrophages to affect kidney function.

Conclusions

The Hippo signaling pathway was inhibited in patients with LN. In the LN mouse model, a reduction in FKN could activate the Hippo signaling pathway, reduce the activation of macrophages in the kidney tissue and polarized these toward the M1 phenotype, thereby reducing renal damage. FKN and the Hippo signaling pathway may become potentially novel molecular targets for the treatment of LN in the future.

Declarations

Acknowledgments

The authors would like to thank Dr Dev Sooranna of Imperial College London for editing the manuscript.

Authors' Contributions

In this work, YZ and XP performed the data analysis, interpreted the results and wrote the manuscript. YY conceived the study, designed the experiments and edited the manuscript. XW contributed to the data collection and commented on previous versions of the manuscript. All the authors read and approved the final manuscript.

Funding

This work was supported by the National Natural Science Foundation of China (no. 81860296) and the Natural Science Foundation of Guangxi Province (nos. 2017GXNSFDA198005 and 2018GXNSFAA281038).

Availability of data and materials

The data that support the findings of this study are available from the corresponding author upon reasonable request. The data are not publicly available because our research team is still conducting follow-up studies related the research.

Ethics approval and consent to participate

The study was approved by the Affiliated Hospital Ethics Committee of Youjiang Medical University for Nationalities (Baise, Guangxi Province, P.R. China) and informed consent was obtained from all participants. For human study,all methods were carried out in accordance with relevant guidelines and regulations. This study was approved by the Ethics Committee of Youjiang Medical University for Nationalities and carried out in compliance with the Animals in Research: Reporting In vivo Experiments

(ARRIVE) guidelines. All animal procedures were in accordance with the Guide for the Care and Use of Laboratory Animals (NIH Publication No. 85–23, revised 1996).

Consent for publication

Not applicable.

Competing interests

The authors declare that they have no competing interests.

References

1. Stojan G, Petri M. Epidemiology of systemic lupus erythematosus: an update. Curr Opin Rheumatol. 2018;30(2):144-50.
2. Anders HJ, Saxena R, Zhao MH, Parodis I, Salmon JE, Mohan C. Lupus nephritis. Nat Rev Dis Primers. 2020;6(1):7.
3. Kiriakidou M, Ching CL. Systemic Lupus Erythematosus. Ann Intern Med. 2020;172(11):Itc81-itc96.
4. Bashford-Rogers RJM, Bergamaschi L, McKinney EF, Pombal DC, Mescia F, Lee JC, et al. Analysis of the B cell receptor repertoire in six immune-mediated diseases. Nature. 2019;574(7776):122-6.
5. Hu L, Hu J, Chen L, Zhang Y, Wang Q, Yang X. Interleukin-22 From Type 3 Innate Lymphoid Cells Aggravates Lupus Nephritis by Promoting Macrophage Infiltration in Lupus-Prone Mice. Front Immunol. 2021;12:584414.
6. Gordon S, Plüddemann A. Macrophage Clearance of Apoptotic Cells: A Critical Assessment. Front Immunol. 2018;9:127.
7. Yunna C, Mengru H, Lei W, Weidong C. Macrophage M1/M2 polarization. Eur J Pharmacol. 2020;877:173090.
8. Wang Y, Smith W, Hao D, He B, Kong L. M1 and M2 macrophage polarization and potentially therapeutic naturally occurring compounds. Int Immunopharmacol. 2019;70:459-66.
9. Korbecki J, Simińska D, Kojder K, Grochans S, Gutowska I, Chlubek D, et al. Fractalkine/CX3CL1 in Neoplastic Processes. Int J Mol Sci. 2020;21(10).
10. Chan HC, Chan HC, Liang CJ, Lee HC, Su H, Lee AS, et al. Role of Low-Density Lipoprotein in Early Vascular Aging Associated With Systemic Lupus Erythematosus. Arthritis Rheumatol. 2020;72(6):972-84.
11. You Y, Qin Y, Lin X, Yang F, Wang J, Yuan F, et al. Upregulated fractalkine levels in Chinese patients with lupus nephritis. Cytokine. 2018;104:23-8.
12. Sharif AAD, Hergovich A. The NDR/LATS protein kinases in immunology and cancer biology. Semin Cancer Biol. 2018;48:104-14.
13. Bae SJ, Luo X. Activation mechanisms of the Hippo kinase signaling cascade. Biosci Rep. 2018;38(4).

14. Yamauchi T, Moroishi T. Hippo Pathway in Mammalian Adaptive Immune System. Cells. 2019;8(5).
15. Mazzone R, Zwergel C, Artico M, Taurone S, Ralli M, Greco A, et al. The emerging role of epigenetics in human autoimmune disorders. Clin Epigenetics. 2019;11(1):34.
16. Gong Q, Jiang Y, Pan X, You Y. Fractalkine aggravates LPS-induced macrophage activation and acute kidney injury via Wnt/β-catenin signalling pathway. J Cell Mol Med. 2021;25(14):6963-75.
17. Durcan L, O'Dwyer T, Petri M. Management strategies and future directions for systemic lupus erythematosus in adults. Lancet. 2019;393(10188):2332-43.
18. Raimbourg Q, Daugas É. [Lupus nephritis]. Nephrol Ther. 2019;15(3):174-89.
19. Ma R, Jiang W, Li Z, Sun Y, Wei Z. Intrarenal macrophage infiltration induced by T cells is associated with podocyte injury in lupus nephritis patients. Lupus. 2016;25(14):1577-86.
20. Wang C, Zou WZ, Zheng X, E J, Wang SX, Zhao MH, et al. [Cellular components of crescents in four common types of crescentic glomerulonephritis]. Zhonghua Bing Li Xue Za Zhi. 2011;40(1):37-41.
21. Lee S, Huen S, Nishio H, Nishio S, Lee HK, Choi BS, et al. Distinct macrophage phenotypes contribute to kidney injury and repair. J Am Soc Nephrol. 2011;22(2):317-26.
22. Chalmers SA, Chitu V, Ramanujam M, Putterman C. Therapeutic targeting of macrophages in lupus nephritis. Discov Med. 2015;20(108):43-9.
23. Carvalho-Pinto CE, García MI, Mellado M, Rodríguez-Frade JM, Martín-Caballero J, Flores J, et al. Autocrine production of IFN-gamma by macrophages controls their recruitment to kidney and the development of glomerulonephritis in MRL/lpr mice. J Immunol. 2002;169(2):1058-67.
24. Kulkarni O, Pawar RD, Purschke W, Eulberg D, Selve N, Buchner K, et al. Spiegelmer inhibition of CCL2/MCP-1 ameliorates lupus nephritis in MRL-(Fas)lpr mice. J Am Soc Nephrol. 2007;18(8):2350-8.
25. Gupta R, Yadav A, Aggarwal A. Urinary soluble CD163 is a good biomarker for renal disease activity in lupus nephritis. Clin Rheumatol. 2021;40(3):941-8.
26. Yoneda O, Imai T, Goda S, Inoue H, Yamauchi A, Okazaki T, et al. Fractalkine-mediated endothelial cell injury by NK cells. J Immunol. 2000;164(8):4055-62.
27. Jones B, Koch AE, Ahmed S. Pathological role of fractalkine/CX3CL1 in rheumatic diseases: a unique chemokine with multiple functions. Front Immunol. 2011;2:82.
28. Li F, Zhang H, Xu KY, Wei Q, Zhou GX. Role of the chemokine fractalkine in a rat model of acute necrotizing pancreatitis and the interventional effect of ulinastatin. Arch Iran Med. 2013;16(2):83-7.
29. Chu L, Li X, Yu W, Qian T, Qi H, Huang L, et al. Expression of fractalkine (CX3CL1) and its receptor in endotoxin-induced uveitis. Ophthalmic Res. 2009;42(3):160-6.
30. Furuichi K, Gao JL, Murphy PM. Chemokine receptor CX3CR1 regulates renal interstitial fibrosis after ischemia-reperfusion injury. Am J Pathol. 2006;169(2):372-87.
31. Furuichi K, Wada T, Iwata Y, Sakai N, Yoshimoto K, Shimizu M, et al. Upregulation of fractalkine in human crescentic glomerulonephritis. Nephron. 2001;87(4):314-20.

32. Ma S, Meng Z, Chen R, Guan KL. The Hippo Pathway: Biology and Pathophysiology. Annu Rev Biochem. 2019;88:577-604.
33. Song J, Wang T, Chi X, Wei X, Xu S, Yu M, et al. Kindlin-2 Inhibits the Hippo Signaling Pathway by Promoting Degradation of MOB1. Cell Rep. 2019;29(11):3664-77.e5.
34. Feng J, Li H, Zhang Y, Wang Q, Zhao S, Meng P, et al. Mammalian STE20-Like Kinase 1 Deletion Alleviates Renal Ischaemia-Reperfusion Injury via Modulating Mitophagy and the AMPK-YAP Signalling Pathway. Cell Physiol Biochem. 2018;51(5):2359-76.
35. Xu J, Li PX, Wu J, Gao YJ, Yin MX, Lin Y, et al. Involvement of the Hippo pathway in regeneration and fibrogenesis after ischaemic acute kidney injury: YAP is the key effector. Clin Sci (Lond). 2016;130(5):349-63.
36. Guo P, Wang Z, Zhou Z, Tai Y, Zhang A, Wei W, et al. Immuno-hippo: Research progress of the hippo pathway in autoimmune disease. Immunol Lett. 2021;230:11-20.
37. Ji X, Song L, Sheng L, Gao A, Zhao Y, Han S, et al. Cyclopeptide RA-V Inhibits Organ Enlargement and Tumorigenesis Induced by YAP Activation. Cancers (Basel). 2018;10(11).

Figures

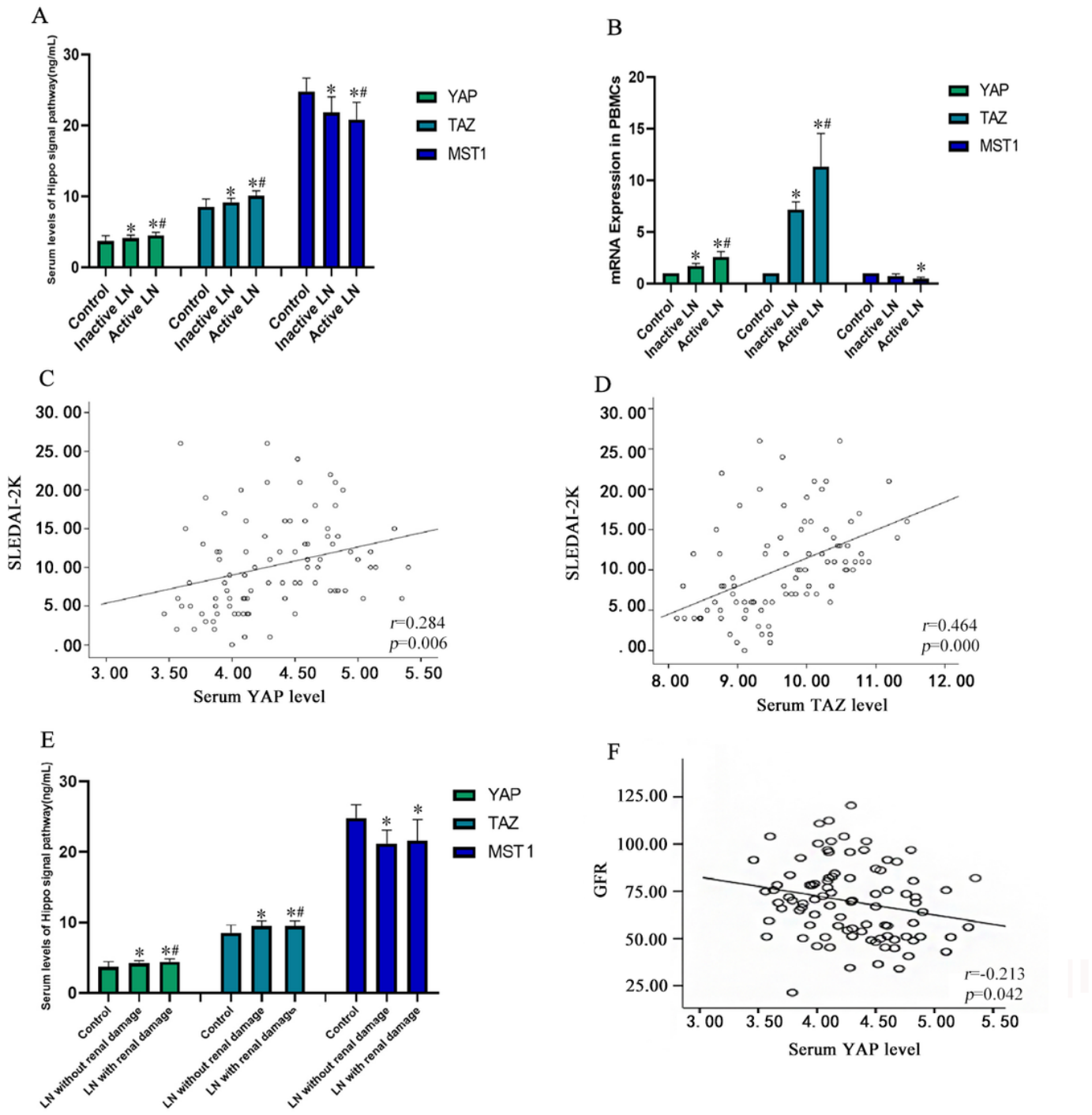

Figure 1

The Hippo signaling pathway was inhibited in LN patients and correlated with disease severity and renal impairment.

A, ELISAs were performed to measure the serum levels of YAP, TAZ and MST1 in healthy controls (n=64), inactive LN patients (n=45) and active LN patients (n=46) respectively. B, RT-qPCR was performed to quantify the expression levels of mRNA in healthy controls (n=64), inactive LN patients (n=45) and active

LN patients (n=46) respectively. *P<0.01 when compared with the control group; #P<0.05 when compared with inactive LN. C, a positive correlation between YAP serum expression levels and SLEDAI-2K in patients with LN (n=91). D, a positive correlation between serum TAZ levels and SLEDAI-2K in patients with LN (n=91). E**,** ELISAs were performed to measure the serum levels of YAP, TAZ and MST in healthy controls (n=64), LN patients without renal damage (n=41) and LN patients with renal damage (n=50) respectively. *p<0.01 when compared with control group; #p<0.05 when compared with LN patients without renal damage. F, Negative correlation between serum YAP levels and GFR in patients with LN (n=91).

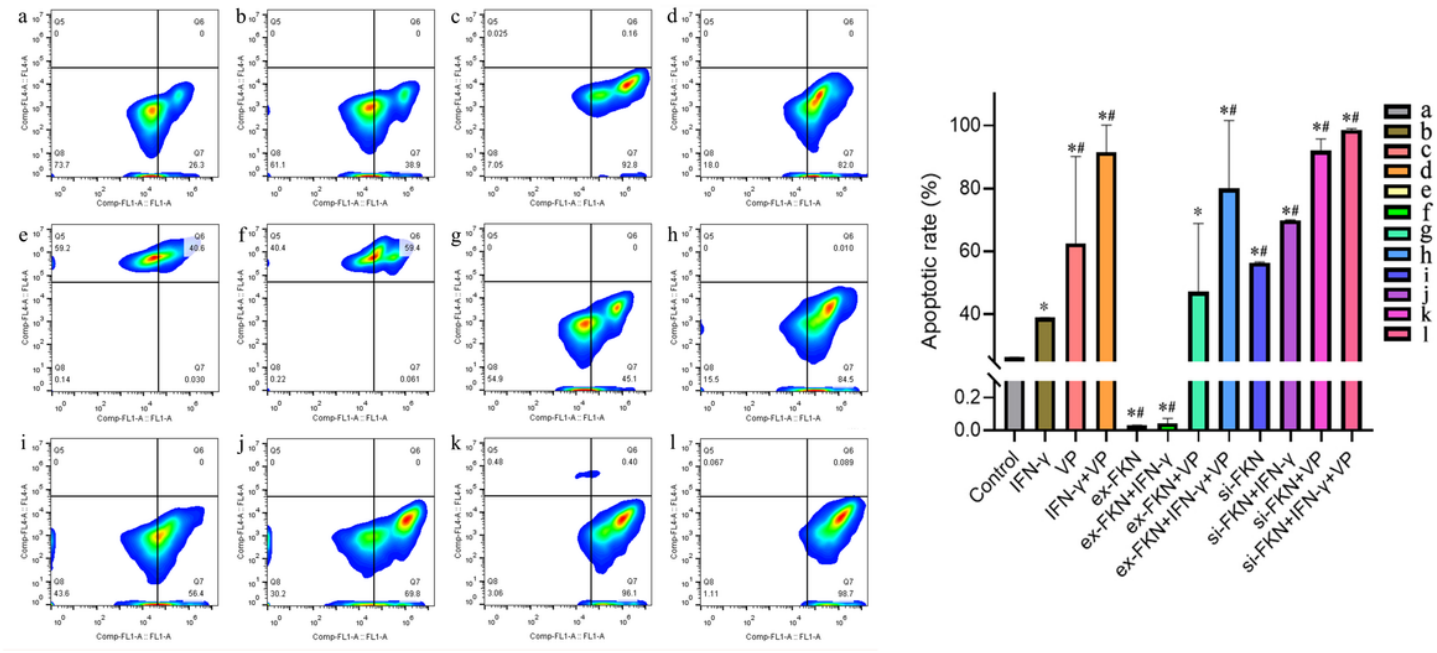

Figure 2

FKN inhibited the apoptosis of RAW264.7 macrophages via the Hippo signaling pathway.

*P<0.05 when compared with the control group; #P <0.05 when compared with the IFN-γ group.

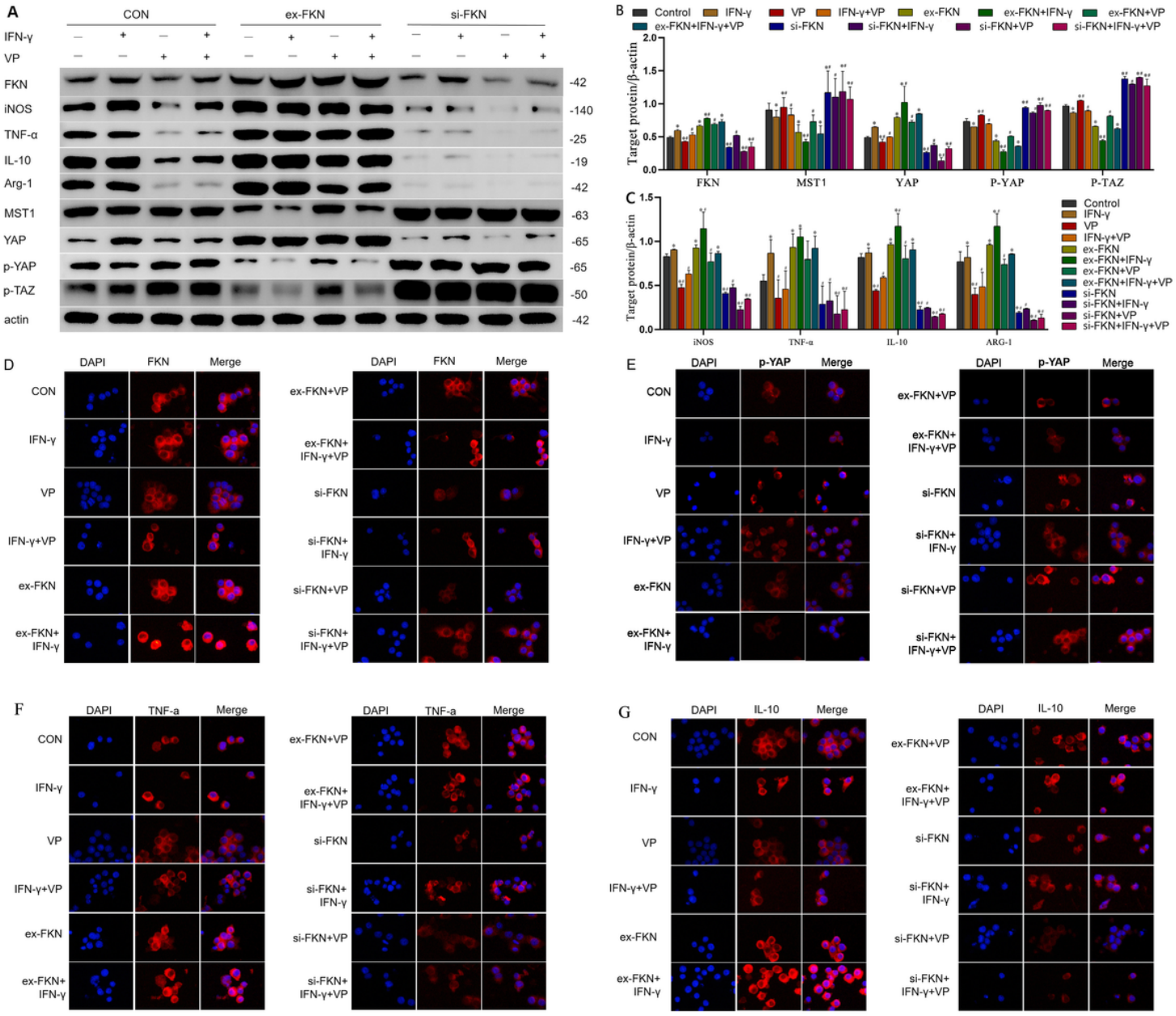

Figure 3

FKN regulated polarization in IFN-γ-induced RAW264.7 cells via the Hippo signaling pathway.

A, B, C, Western blot analysis and their respective quantitation were performed to assess the expression levels of FKN, MST1, YAP, p-YAP, p-TAZ, iNOS, TNF-α, Arg-1 and IL-10 protein in RAW264.7 cells(full-length blots are presented in Supplementary Figure1). Representative blots are shown. *P<0.05 when compared with the control group; $^{\#}P$<0.05 when compared with the IFN-γ group. D-G, Immunofluorescence analysis was used to ascertained the subcellular localization of FKN, p-YAP, IL-10 and TFN-α. Representative photomicrographs are shown.

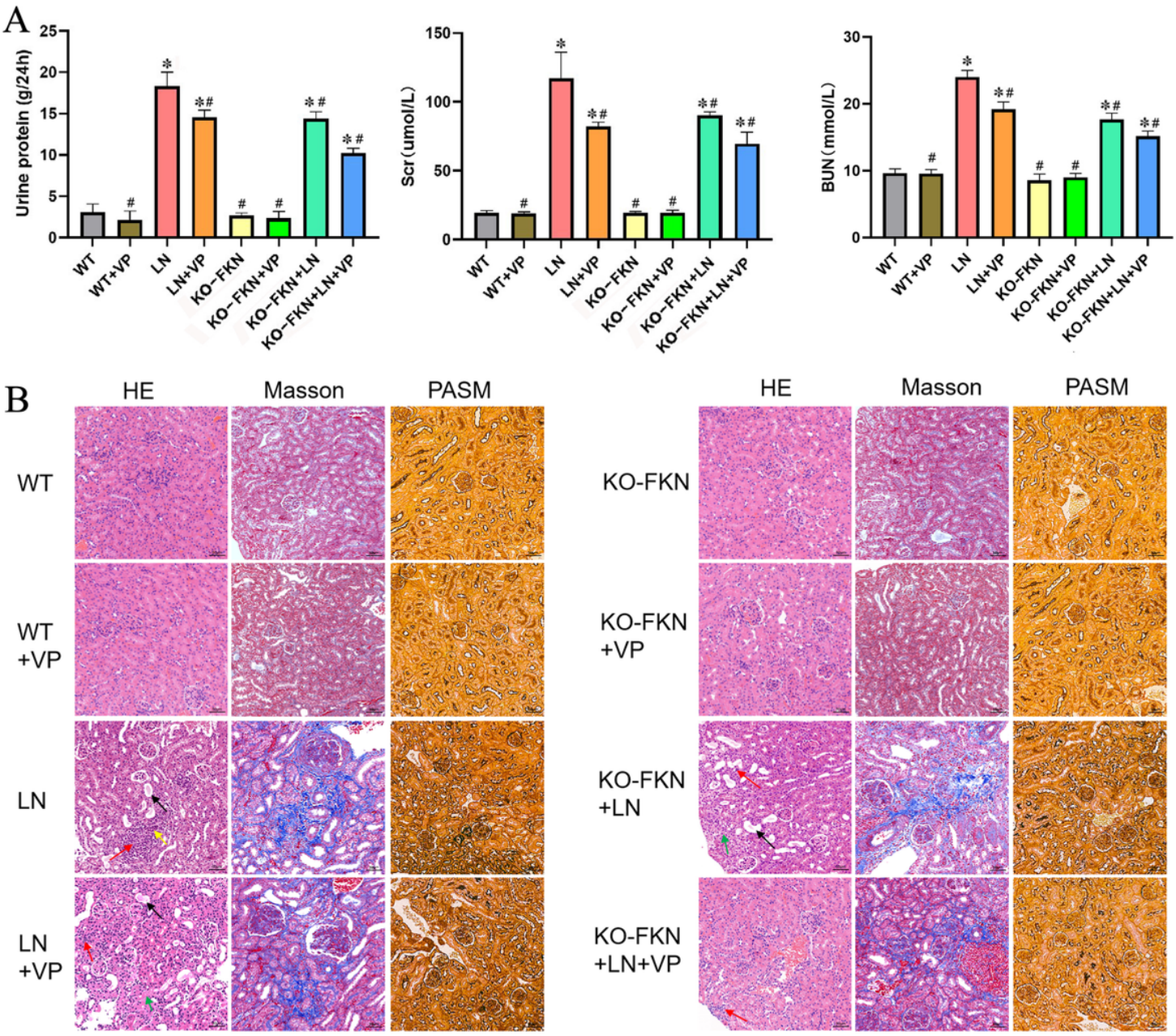

Figure 4

FKN deficiency attenuated the renal damage of LN via activation of the Hippo signaling pathway.

A, The BUN, serum creatinine and 24 h urinary protein levels. B show HE, Masson and PASM staining of kidney tissues. $^{*}P<0.05$ when compared with the WT Mice; $^{\#}P<0.05$ when compared with the LN Mice. (Red arrows: inflammatory cell infiltration in the interstitium; yellow arrows: abscesses and a large number of necrotic neutrophils in the lumen of some renal tubules; black arrows: dilated tubules and protein deposits; green arrows: degenerated renal tubules and the epithelial cell cytoplasm was loose). Representative photomicrographs are shown.

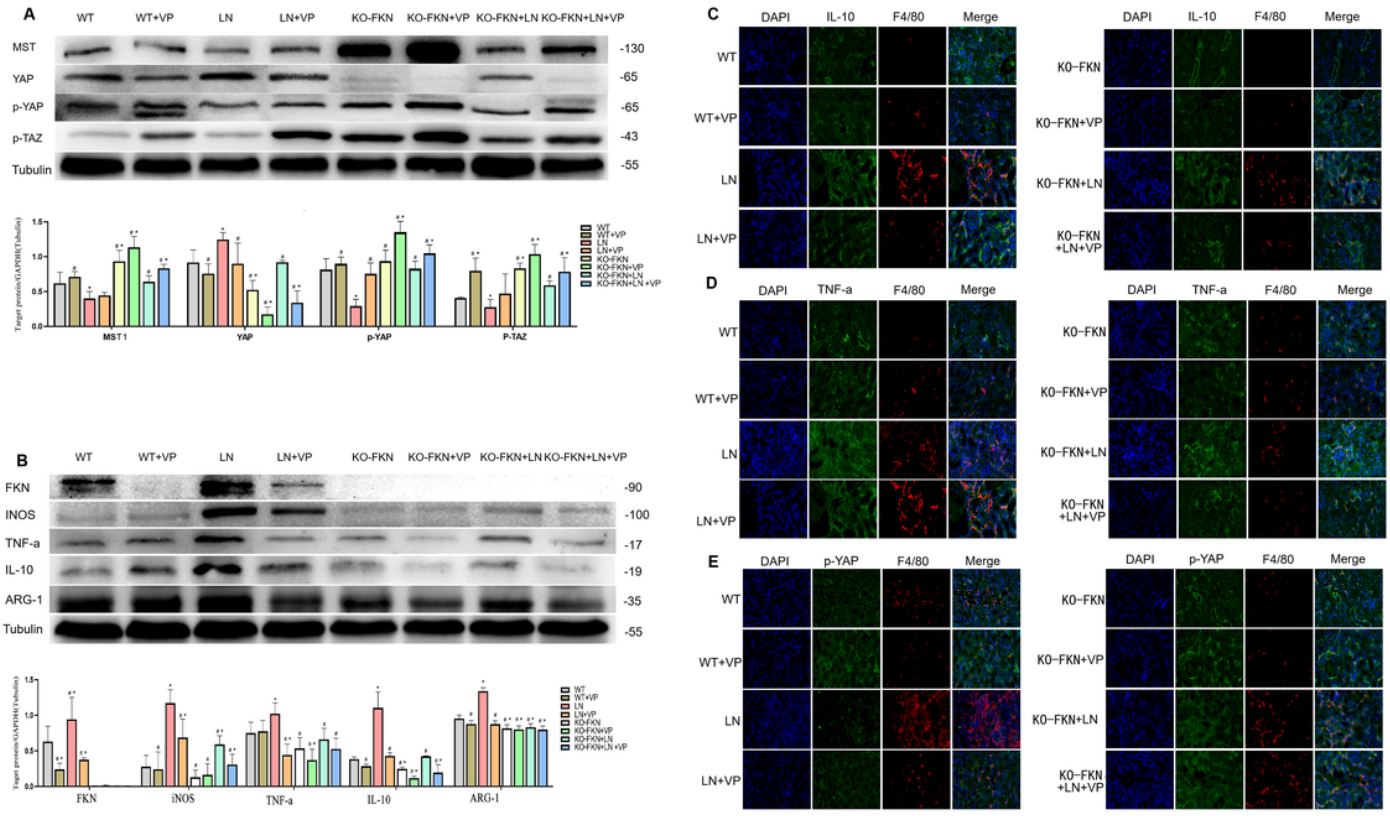

Figure 5

FKN deficiency suppressed macrophages polarization and proliferation in mice kidney tissues via activation of the Hippo signaling pathway.

A Western blot analysis and their respective quantitation showing the protein expression levels of MST1, YAP, p-YAP, p-TAZ, in mice kidney tissues(full-length blots are presented in Supplementary Figure2). B Western blot analysis and their respective quantitation showing the protein expression levels of FKN, iNOS, TNF-α, Arg-1 and IL-10 in mice kidney tissues(full-length blots are presented in Supplementary Figure3). Representative blots are shown. $^{*}P < 0.05$ when compared with the WT mice; $^{\#}P < 0.05$ when compared with the LN mice. C, D and E show F4/80, p-YAP, IL-10 and TNF-a protein localization in mice kidney tissues. Representative photomicrographs are shown.

Supplementary Files

This is a list of supplementary files associated with this preprint. Click to download.

- SupplementaryFigure1.tif
- SupplementaryFigure2.tif
- SupplementaryFigure3.tif